Check for updates

Received: 20 March 2020 | Revised: 15 May 2020 | Accepted: 8 June 2020

DOI: 10.1111/ajt.16148

ORIGINAL ARTICLE

AJT

Lysis of cold-storage-induced microvascular obstructions for ex vivo revitalization of marginal human kidneys

Jenna R. DiRito[1,2] | Sarah A. Hosgood[1] | Melanie Reschke[3] | Claire Albert[4] | Laura G. Bracaglia[4] | John R. Ferdinand[5] | Benjamin J. Stewart[5] | Christopher M. Edwards[2] | Anand G. Vaish[2] | Sathia Thiru[6] | David C. Mulligan[2] | Danielle J. Haakinson[2] | Menna R. Clatworthy[5] | W. Mark Saltzman[4] | Jordan S. Pober[7] | Michael L. Nicholson[1] | Gregory T. Tietjen[2,4]

[1]Department of Surgery, University of Cambridge, Cambridge, UK

[2]Department of Surgery, Yale School of Medicine, New Haven, Connecticut

[3]Department of Molecular Biophysics & Biochemistry, Yale University, New Haven, Connecticut

[4]Department of Biomedical Engineering, Yale University, New Haven, Connecticut

[5]Molecular Immunity Unit, Department of Medicine, University of Cambridge, Cambridge, UK

[6]Department of Pathology, University of Cambridge, Cambridge, UK

[7]Department of Immunobiology, Yale University, New Haven, Connecticut

Correspondence
Gregory T. Tietjen
Email: gregory.tietjen@yale.edu

Michael L. Nicholson
Email: mln31@cam.ac.uk

Funding information
US National Institutes of Health, Grant/Award Number: U01-AI32895 and R01-DK124420; New England Donor Services; National Institute for Health Research Blood and Transplant Research Unit

Thousands of kidneys from higher-risk donors are discarded annually because of the increased likelihood of complications posttransplant. Given the severe organ shortage, there is a critical need to improve utilization of these organs. To this end, normothermic machine perfusion (NMP) has emerged as a platform for ex vivo assessment and potential repair of marginal organs. In a recent study of 8 transplant-declined human kidneys on NMP, we discovered microvascular obstructions that impaired microvascular blood flow. However, the nature and physiologic impact of these lesions were unknown. Here, in a study of 39 human kidneys, we have identified that prolonged cold storage of human kidneys induces accumulation of fibrinogen within tubular epithelium. Restoration of normoxic conditions—either ex vivo during NMP or in vivo following transplant—triggered intravascular release of fibrinogen correlating with red blood cell aggregation and microvascular plugging. Combined delivery of plasminogen and tissue plasminogen activator during NMP lysed the plugs leading to a significant reduction in markers of renal injury, improvement in indicators of renal function, and improved delivery of vascular-targeted nanoparticles. Our study suggests a new mechanism of cold storage injury in marginal organs and provides a simple treatment with immediate translational potential.

KEYWORDS

basic (laboratory) research/science, coagulation and hemostasis, disease pathogenesis, kidney biology, kidney transplantation/nephrology, thrombolytic therapy/thrombolysis, translational research/science, vascular biology

Abbreviations: Ab, antibody; DBD, donor after brain death; DCD, donor after cardiac death; ICAM2, intercellular adhesion molecule 2; MSB, martius scarlet blue; NMP, normothermic machine perfusion; NPs, nanoparticles; PLA-PEG, poly[lactic acid]-poly[ethylene-glycol]; RBCs, red blood cells; RBF, renal blood flow; TEM, transmission electron microscopy; tPA, tissue plasminogen activator.

Michael L. Nicholson and Gregory T. Tietjen contributed equally to this work.

© 2020 The American Society of Transplantation and the American Society of Transplant Surgeons

16006143, 2021, 1, Downloaded from https://onlinelibrary.wiley.com/doi/10.1111/ajt.16148, Wiley Online Library on [25/10/2022]. See the Terms and Conditions (https://onlinelibrary.wiley.com/terms-and-conditions) on Wiley Online Library for rules of use; OA articles are governed by the applicable Creative Commons License

1 | INTRODUCTION

The current shortage of donor organs leads to an average of 13 deaths on the kidney waitlist each day.[1] In the same 24-hour period, ~10 donated kidneys are declined for transplant and ultimately discarded without clinical use often because of concerns over post-transplant complications associated with organs from medically complex donors.[2,3] However, the continuing decline in the health of the organ donor population (eg, increasing age, obesity) suggests that discarding all suboptimal organs is not a viable long-term strategy.[4-7] Normothermic machine perfusion (NMP) has emerged as a potential strategy to reduce organ discard by improving viability assessment and further enabling therapeutic intervention to revitalize marginal organs.

In the current clinical practice of NMP, blood flow is reestablished throughout the organ using serum-depleted red-blood-cells (RBCs) at or near body temperature for 1 hour prior to transplantation.[8] This approach has been established as a safe clinical procedure and a randomized control trial is currently underway to assess if there are direct clinical benefits of NMP alone relative to standard cold preservation in kidneys donated after cardiac death (DCD).[8-10] In addition to the potential benefits of 1 hour of NMP alone, this approach has significant potential to enable ex vivo delivery of agents intended to repair or modulate organs prior to transplantation.[11] A number of therapeutic approaches across multiple organ types are currently under preclinical evaluation for use during NMP including cellular therapy, gene editing, and nanomedicines.[12-14]

Recently, we have shown that antibody-conjugated nanoparticle drug carriers (NPs) can be targeted to renal vasculature in the context of human kidney NMP.[13] We found that NPs targeting CD31, a pan-endothelial surface protein, could enhance NP retention in well-perfused organs. However, we also identified that NPs tended to accumulate nonspecifically at sites of microvascular plugs that arose to varying degrees in each of 8 human organs evaluated.[13] This phenomenon exacerbated the heterogeneity of NP delivery with many regions of the organ left untreated. In addition, these obstructions impaired microvascular perfusion, likely leading to reduced oxygen and nutrient delivery in the plugged regions.

On the basis of this prior work, we hypothesized that removal of these microvascular plugs during NMP would improve organ viability ex vivo and also potentiate subsequent therapeutic delivery. To evaluate this hypothesis, we first sought to identify the cause of these microvascular obstructions as our prior work had suggested that these were not classical microthrombi. We then endeavored to use this mechanistic knowledge to design and evaluate a therapeutic intervention for delivery during NMP.

2 | MATERIALS AND METHODS

Additional information can be found in Data S1.

2.1 | NMP of transplant-declined kidneys

Use of all human kidneys in this study have been approved by The North East Newcastle & North Tyneside 2 research ethics committee (15/NE/0408), New England Donor Services, the National Health Service (NHS) Health Research Authority East of England, Cambridge Central Research Committee (15/EE/0356, and NHS Research & Development [R&D]). NMP was conducted as previously described;[13] additional details are provided in Data S1.

2.2 | Fibrinogen immunofluorescence, western blot, and ELISA evaluation

Kidney sections were stained with monoclonal mouse antihuman fibrin(ogen) antibody (Ab) (MyBioSource, San Diego, CA) prior to washing and staining with secondary Ab (Alexa Fluor 546 goat anti-mouse IgM, Fischer) and vascular stain (DyLight 649 Ulex). We refer to this as "fibrin(ogen)" here and where appropriate in the rest of the manuscript because this antibody (and all those available to us commercially) cannot distinguish between fibrinogen and the thrombin-cleaved fibrinogen product known as fibrin. However, we assumed that positive intracellular immunostaining was indicative of native fibrinogen as this protein could not have been exposed to thrombin.

After staining, samples were mounted with Vectashield Hard Set mounting media preceding imaging. For ELISA (Abcam, Cambridge, UK) and western blot analysis of fibrin(ogen) levels, biopsies were processed into protein lysates according to established vendor protocols (Abcam, Cambridge, UK). Total protein in the tissue lysate was measured using a Pierce BCA protein assay kit (ThermoFisher, Waltham, MA). Additional information is provided in Data S1.

2.3 | tPA + plasminogen treatment

Plasminogen was added to the perfusate prior to NMP at a final concentration of 10 μg/mL and then allowed to circulate for the first 30 minutes of NMP prior to tissue plasminogen activator (tPA) delivery in treated groups at a dose of 100 μg/kg of graft. This dose was matched to the typical in vivo dosage used clinically for arterial thrombosis. Each organ otherwise underwent a standard clinical course of NMP. In all organs, repeat biopsies were collected at 3 time points: (1) at the end of cold-storage to confirm fibrinogen presence in tubular epithelia, (2) after 30 minutes of NMP to allow translocation into the vasculature, and (3) after an additional 60 minutes of NMP either in the presence of tPA + plasminogen or tPA alone. Additional details of tPA administration and biochemical analysis are provided in Data S1.

16006143, 2021, 1, Downloaded from https://onlinelibrary.wiley.com/doi/10.1111/ajt.16148, Wiley Online Library on [25/10/2022]. See the Terms and Conditions (https://onlinelibrary.wiley.com/terms-and-conditions) on Wiley Online Library for rules of use; OA articles are governed by the applicable Creative Commons License

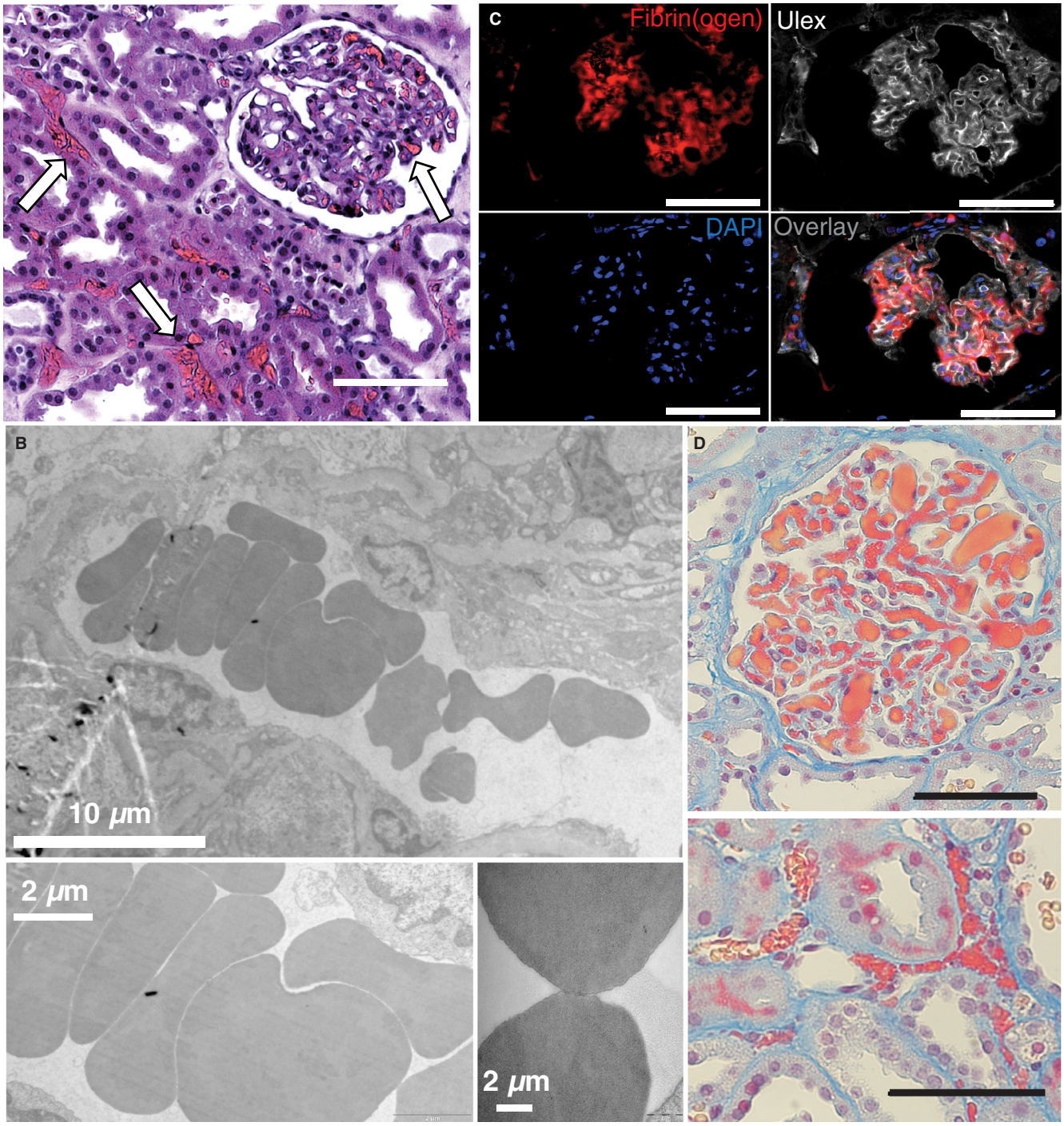


FIGURE 1 Fibrin(ogen)-rich microvascular plugs are present after normothermic machine perfusion (NMP). Representative images from biopsies of perfused human kidneys 30 min after the start of NMP in A, H&E stained samples (white arrows) and B, transmission electron microscopy samples showing microvascular obstructions with a rouleaux-like aggregation of red blood cells (RBCs). C, Fluorescent staining depicts co-localization of fibrin(ogen) (red) with vasculature (white Ulex stain). Nuclei are stained blue. D, Martius scarlet blue (MSB) stained samples (red–fibrin[ogen]; yellow–RBC) showing obstructions in both glomeruli (top) and microvessels (bottom). Scale bars represent 100 μm unless otherwise noted. [Color figure can be viewed at wileyonlinelibrary.com]

2.4 | Quantitative microscopy of microvascular obstructions in paraffin sections

Biopsies were fixed in 10% formalin, paraffin embedded, cut to 4 μm, and stained with a martius scarlet blue (MSB) kit (TCS Biosciences, Buckingham, UK). Though it is classically associated with staining of fibrin, similar to the immunofluorescence, the MSB stain also cannot definitively distinguish between fibrinogen, fibrin monomer, or fully polymerized fibrin.[15,16] However, again similar to the immunofluorescence, we assumed that positive intracellular MSB

16006143, 2021, 1, Downloaded from https://onlinelibrary.wiley.com/doi/10.1111/ajt.16148, Wiley Online Library on [25/10/2022]. See the Terms and Conditions (https://onlinelibrary.wiley.com/terms-and-conditions) on Wiley Online Library for rules of use; OA articles are governed by the applicable Creative Commons License

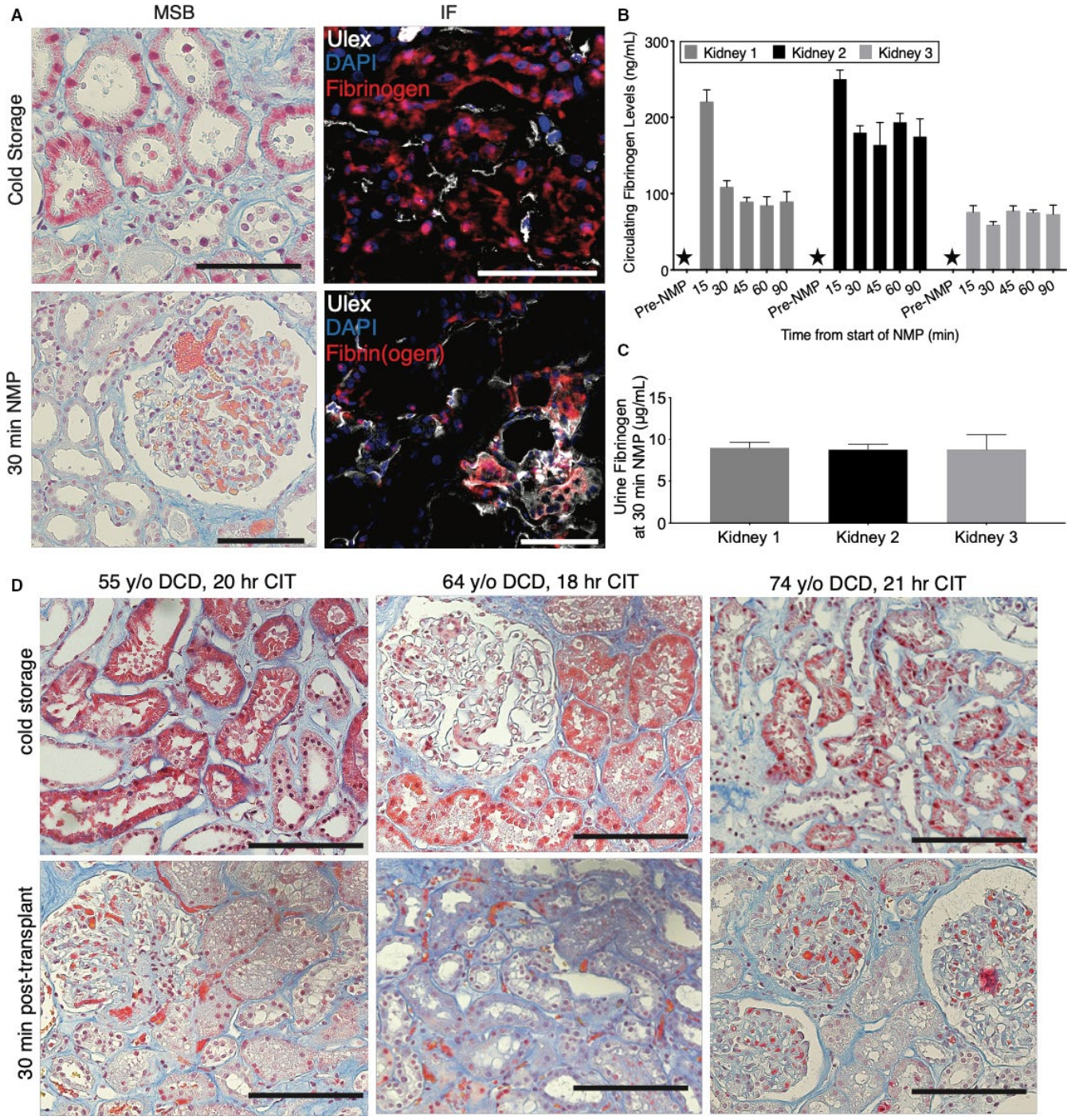


FIGURE 2 Normothermic reperfusion triggers intravascular accumulation of tubular-cell-derived fibrinogen. A, Representative images of biopsies from human kidneys sampled during cold storage (upper panels) demonstrating positive stain in tubular epithelia in both martius scarlet blue (MSB; left; pink stain) and immunofluorescence (right; fibrinogen/fibrin[ogen]–red; Ulex–white; Dapi–blue). A repeat biopsy after 30 min of normothermic machine perfusion (NMP) in the same organ depicts the migration of the positive stain to the vasculature (lower panels). B, Fibrin(ogen) levels in perfusate as measured by ELISA in technical triplicate for samples taken before and during NMP. Stars indicate samples below limit of detection. C, Urine fibrin(ogen) levels in human kidneys measured in technical triplicate at 30 min of NMP. D, Representative images from a clinical cohort of kidneys during cold storage demonstrating positive MSB stain in tubular epithelia with MSB stain (top). A repeat biopsy in the same organ taken 30 min posttransplant depicts the migration of the positive stain to the vasculature (bottom). Scale bars represent 100 µm [Color figure can be viewed at wileyonlinelibrary.com]

stain was indicative of native fibrinogen since this protein could not have been exposed to thrombin; fibrin(ogen) was still used to refer to intravascular MSB stain. For quantification, 20 brightfield images per biopsy were collected on an Olympus IX Series microscope using a custom machine-learning algorithm. Additional details are provided in Data S1.

16006143, 2021, 1, Downloaded from https://onlinelibrary.wiley.com/doi/10.1111/ajt.16148, Wiley Online Library on [25/10/2022]. See the Terms and Conditions (https://onlinelibrary.wiley.com/terms-and-conditions) on Wiley Online Library for rules of use; OA articles are governed by the applicable Creative Commons License

2.5 | Nanoparticle delivery

Intercellular adhesion molecule 2 (ICAM2) targeted-NPs (red) and control-NPs (green) were prepared, delivered, and quantified as previously described.[13] Additional information can be found in Data S1.

3 | RESULTS

3.1 | Fibrin(ogen)-rich microvascular obstructions are present after NMP

We have routinely observed microvascular obstructions in the renal cortex following NMP (Figure 1A).[13] High resolution evaluation by transmission electron microscopy (TEM) showed no evidence of either fibrin mesh or platelets as would be typically associated with either preexisting or newly formed microthrombi (Figure 1B). Instead, the obstructions appeared to be aggregates of RBCs in a rouleaux-like formation (ie, with the appearance of stacked coins).

Immunofluorescence confirmed high levels of fibrin(ogen)-specific staining as would be expected with rouleaux RBC-aggregates in vivo,[17-19] (Figure 1C; Figure S1). To simultaneously visualize the fibrin(ogen) and RBCs within microvascular obstructions, an MSB trichrome stain was employed (Figure 1D). The MSB staining revealed dense aggregates of apparent fibrin(ogen) (red) and RBCs (yellow) in both peritubular capillaries and glomeruli.

3.2 | Normothermic reperfusion triggers intravascular accumulation of tubular-cell-derived fibrinogen

As our perfusate lacks serum proteins (including fibrinogen), we anticipated that the fibrin(ogen)-rich obstructions must have formed in the donor when circulating fibrinogen derived from the liver was present. To assess this, we evaluated repeat kidney biopsies taken from the same donor organ prior to NMP (ie, at the end point of cold storage) and then again after 30 minutes of NMP (Figure 2A). Surprisingly, we found that the fibrinogen stain was initially localized within proximal tubular epithelium during cold storage. Here we presume that this intracellular fibrinogen could not have been exposed to any extracellular thrombin for conversion to fibrin. Thus, we refer to this intracellular protein specifically as "fibrinogen" and not "fibrin(ogen)," which we reserve to describe the intravascular protein where thrombin cleavage is at least theoretically possible. This epithelial stain was lost after 30 minutes of NMP and coincided with the appearance of intravascular fibrin(ogen) concentrated at sites of microvascular obstruction (Figure 2A).

ELISA analysis confirmed that there was no soluble fibrin(ogen) in the perfusate prior to NMP, but soluble fibrin(ogen) became detectable as early as 15 minutes following commencement of NMP (Figure 2A,B). Notably, we detected no measurable thrombin activity in the perfusate as expected given the absence of serum proteins. This finding further supports the hypothesis that these microvascular obstructions are not classical microthrombi (Figure S2). Soluble fibrin(ogen) was also detected at high levels in the urine produced during NMP (Figure 2C); urine is not recirculated in our system. The levels of soluble fibrin(ogen) appeared much higher in urine than in the perfusate. However, the measurement of circulating fibrin(ogen) in the perfusate does not account for insoluble fibrin(ogen) contained within the microvascular obstructions preventing direct comparison.

To assess if this process of fibrinogen secretion would occur in a clinical setting, we evaluated a cohort of 15 human kidneys before and after clinical transplantation (Table S1).[8] These 15 donor organs represent the first sequential organs that had both pretransplant and 30 minutes posttransplant biopsies from the control arm of an ongoing randomized control trial in the United Kingdom (ISRCTN15821205). Thus, the kidneys in this cohort varied in age and underwent variable periods of cold-storage time (Table S1). Positive MSB stain was observed prior to transplant in the tubular epithelium of 6 of the 15 kidneys (Figure S3). Similar to our findings during NMP, this epithelial stain was lost 30 minutes posttransplant and coincided with the presence of positive intravascular stain colocalized with microvascular obstructions (Figure 2D).

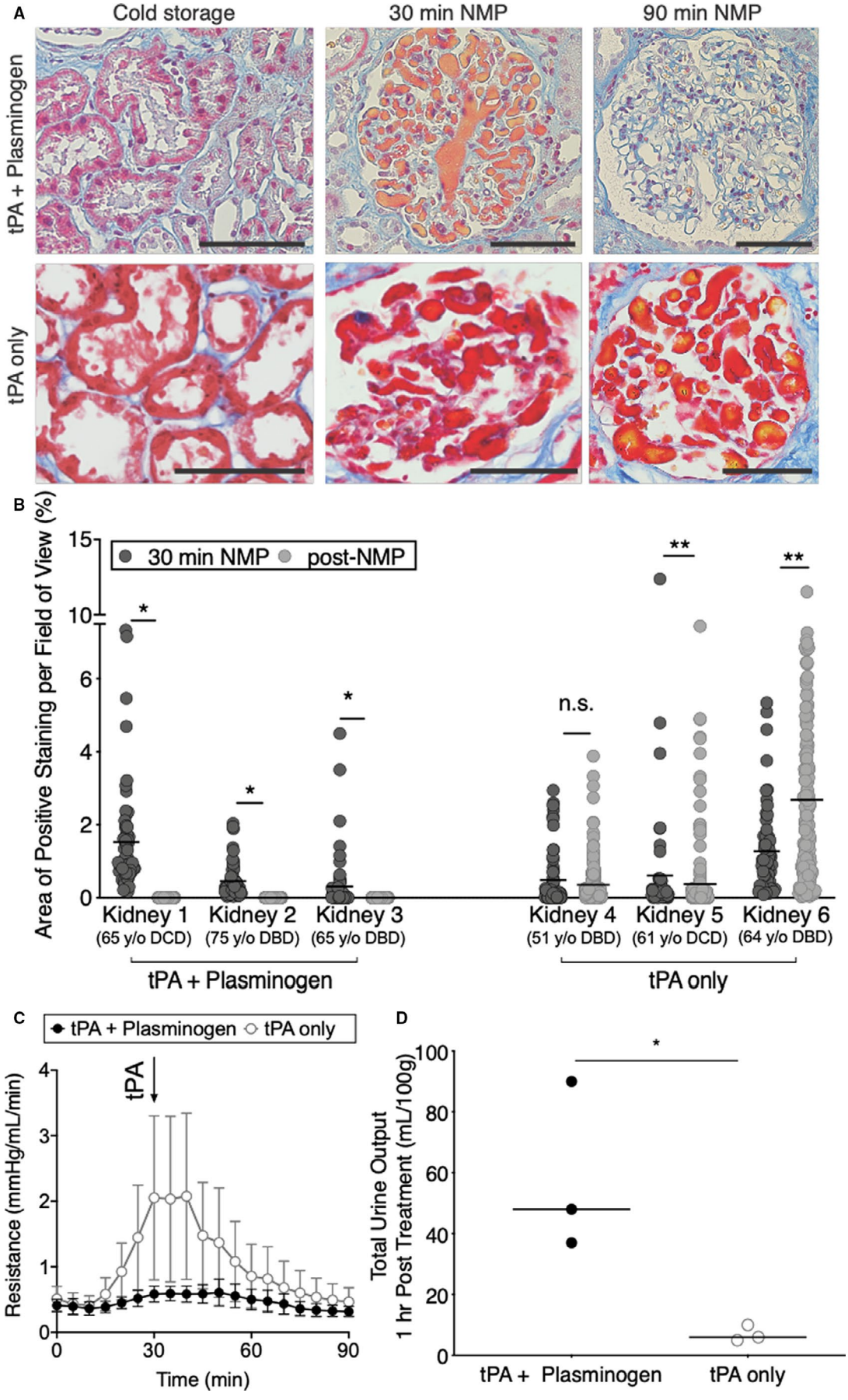
3.3 | Combined tPA + plasminogen treatment lyses microvascular obstructions

Having identified that NMP can initiate exposure of tubular fibrinogen within the vascular lumen, we next evaluated if a fibrinolytic therapy could clear the microvascular obstructions during NMP. We chose a regimen of tPA in combination with its cofactor plasminogen because both are clinically available and would allow for rapid translation. As our perfusate lacks serum proteins—and therefore contains no plasminogen—we hypothesized that exogenous plasminogen would be required for full effect of tPA.

To evaluate this, a series of 6 human kidneys declined for transplantation were evaluated in Study Group 1. The 6 sequential donor kidneys were randomized to receive either treatment with combined tPA + plasminogen or tPA alone. Donor demographics (age, cold-storage time, and reason for transplant decline) are provided in Table S2. Five of the 6 organs in Study Group 1 displayed clearly positive MSB stain of the tubular epithelia in the cold-storage biopsy prior to NMP (Figure 3A; Figure S4). However, all 6 organs displayed measurable levels of microvascular obstructions following the initial 30 minutes of NMP (Figure 3A).

A custom machine-learning algorithm was used to quantify the % area of microvascular obstruction identified by the MSB stain in a series of images from each biopsy (Figures S5-S7). Although levels of microvascular obstructions were variable prior to treatment, 1 hour of treatment with tPA + plasminogen completely cleared microvascular obstructions in all 3 kidneys regardless of the initial degree of microvascular obstruction (*P < .0001; Figure 3A,B). Administration of tPA

16006143, 2021, 1, Downloaded from https://onlinelibrary.wiley.com/doi/10.1111/ajt.16148, Wiley Online Library on [25/10/2022]. See the Terms and Conditions (https://onlinelibrary.wiley.com/terms-and-conditions) on Wiley Online Library for rules of use; OA articles are governed by the applicable Creative Commons License



16006143, 2021, 1, Downloaded from https://onlinelibrary.wiley.com/doi/10.1111/ajt.16148, Wiley Online Library on [25/10/2022]. See the Terms and Conditions (https://onlinelibrary.wiley.com/terms-and-conditions) on Wiley Online Library for rules of use; OA articles are governed by the applicable Creative Commons License

FIGURE 3 Combined tissue plasminogen activator (tPA) + plasminogen treatment lyses microvascular obstructions. A, Representative images and B, quantification of area of microvascular obstruction are shown for single kidneys treated with tPA + plasminogen or tPA only (*P < .0001, **P < .05; Mann-Whitney t test). Scale bars represent 100 μm. C, Resistance time traces as measured during normothermic machine perfusion (NMP) for tPA + plasminogen treated kidneys vs tPA only controls. Data points represent the mean and error bars signify standard error of the mean for each group of 3 kidneys. Arrow denotes point of tPA administration. D, Total urine output normalized to the mass of each kidney as measured after 90 min of NMP (*P = .0340; unpaired t tests). Data points represent individual kidneys [Color figure can be viewed at wileyonlinelibrary.com]

alone did not clear the obstructions (Figure 3A,B) and actually displayed increased levels in 2 of the 3 organs evaluated. An experienced renal pathologist confirmed these findings through blinded assessment of a series of slides across a random sample of organs (Table S3).

Though the organs in this sequential series were not matched for demographic characteristics, we nevertheless assessed indicators of physiologic function. Vascular resistance spiked to higher levels in the tPA only group at ~30-60 minutes of NMP (Figure 3C). In contrast, the tPA + plasminogen group displayed more stable resistance throughout NMP. Although the tPA + plasminogen group appeared to diverge from the controls prior to addition of tPA, it should be noted that plasminogen was in circulation from time 0 and endogenous renal production of tPA is a known phenomenon.[20] In addition to the more stable hemodynamics, the tPA + plasminogen group also produced significantly more urine than controls (Figure 3D).

3.4 | Paired donor organs suggest tPA + plasminogen improves organ viability

To further test the effect of this treatment on organ viability, we evaluated 3 sequential pairs of transplant-declined organs recovered from 3 separate deceased donors in Study Group 2 (Figure 4B). Paired organs from the same donor were used to control for donor to donor variability and differences in cold-storage times. The 3 donors were aged 75 (Pair 1), 63 (Pair 2), and 77 (Pair 3) and were declined for suspected malignancy, biopsy score, and patient refusal respectively (Table S2). Cold storage times ranged from 28 to 34 hours and the cohort included 2 DCD donors (Pairs 1 and 3) and 1 donor after brain death (DBD donor) (Pair 2). Plasminogen was chosen as the negative control for Study Group 2 to evaluate if the exogenous tPA was necessary or if endogenous tPA produced by the kidney was sufficient for full therapeutic effect.

Quantification of the microvascular obstructions revealed donor-to-donor variation in the initial levels of obstructions; the DCD donors (Pairs 1 and 3) had significantly higher initial levels of obstruction compared to the DBD donor (Pair 2). Regardless of the initial level of obstruction, combined tPA + plasminogen treatment again completely eliminated all microvascular obstructions (Figure 4A,B). By contrast, plasminogen alone led to only a minor reduction in Pairs 1 and 3 with high levels of microvascular obstruction remaining in all organs at the end of the NMP course. Biochemical analysis of active plasmin and fibrin(ogen) degradation products in the perfusate further confirmed these results (Figure S8).

We next assessed parameters of physiologic function and organ injury in the treated organs relative to the paired controls. Treated organs again demonstrated more stable vascular resistance as compared to nontreated organs that had a characteristic spike in resistance between ~30-60 minutes (Figure 4C). The volume of urine production was also higher in the treated organs by an average of 2.3-fold ±0.6, though this did not reach statistical significance with only 3 pairs of kidneys (Figure 4D; P = .1582). NGAL, a marker of acute kidney injury, was significantly reduced in the treated kidneys compared to the paired controls (Figure 4E). Finally, we measured changes in protein levels of soluble ICAM-1 and interleukin-6 (IL-6) from pre to post NMP as indicators of vascular injury and inflammation respectively.[21-23] Both ICAM-1 and IL-6 were reduced by significant levels in the tPA + plasminogen group compared to controls (Figure 4F,G).

3.5 | Tubular epithelia produce fibrinogen during cold storage at variable rates depending on the donor

The donor organs from the clinical series evaluated above displayed positive MSB stain in 6/15 kidneys (40%) prior to transplant. This ratio rose to 11/12 kidneys (92%) with positive MSB stain in cold storage for Study Groups 1 and 2 with 12/12 demonstrating microvascular plugging post NMP. Notably, the cold-storage times of the 6 MSB positive kidneys in the clinical cohort was significantly longer than that of the MSB negative organs (Figure S9). The cold-storage times of the transplant-declined research organs were even longer suggesting that this may be a determining factor in renal fibrinogen levels. Based on this evidence, we hypothesized that fibrinogen levels rise during cold storage.

To test this hypothesis, repeat tissue biopsies were collected from a 52-year-old DBD donor organ (Kidney 7; Study Group 3) at 24 and 48 hours of cold storage time and evaluated by western blot for the fibrinogen gamma subunit (52 kDal). An increase in fibrinogen levels was observed at 48 compared to 24 hours (Figure 5A). To further substantiate this finding, a series of 5 transplant-declined human organs (Study Group 3) were obtained early in cold storage (6-12 hours) and subsequently stored for prolonged cold periods with repeat biopsies collected out to 72 hours. Two organs from younger donors (Kidney 8 from a 49-year-old DBD and Kidney 9 from a 39-year-old DCD) were negative for MSB stain at the earliest time of 12 hours. However, the MSB staining showed a clear time-dependent increase in tubular staining out to 72 hours (Figure 5B). ELISA performed on tissue lysates also demonstrated a linear increase of fibrinogen levels during this period consistent with the MSB staining (Figure 5C).

16006143, 2021, 1, Downloaded from https://onlinelibrary.wiley.com/doi/10.1111/ajt.16148, Wiley Online Library on [25/10/2022]. See the Terms and Conditions (https://onlinelibrary.wiley.com/terms-and-conditions) on Wiley Online Library for rules of use; OA articles are governed by the applicable Creative Commons License

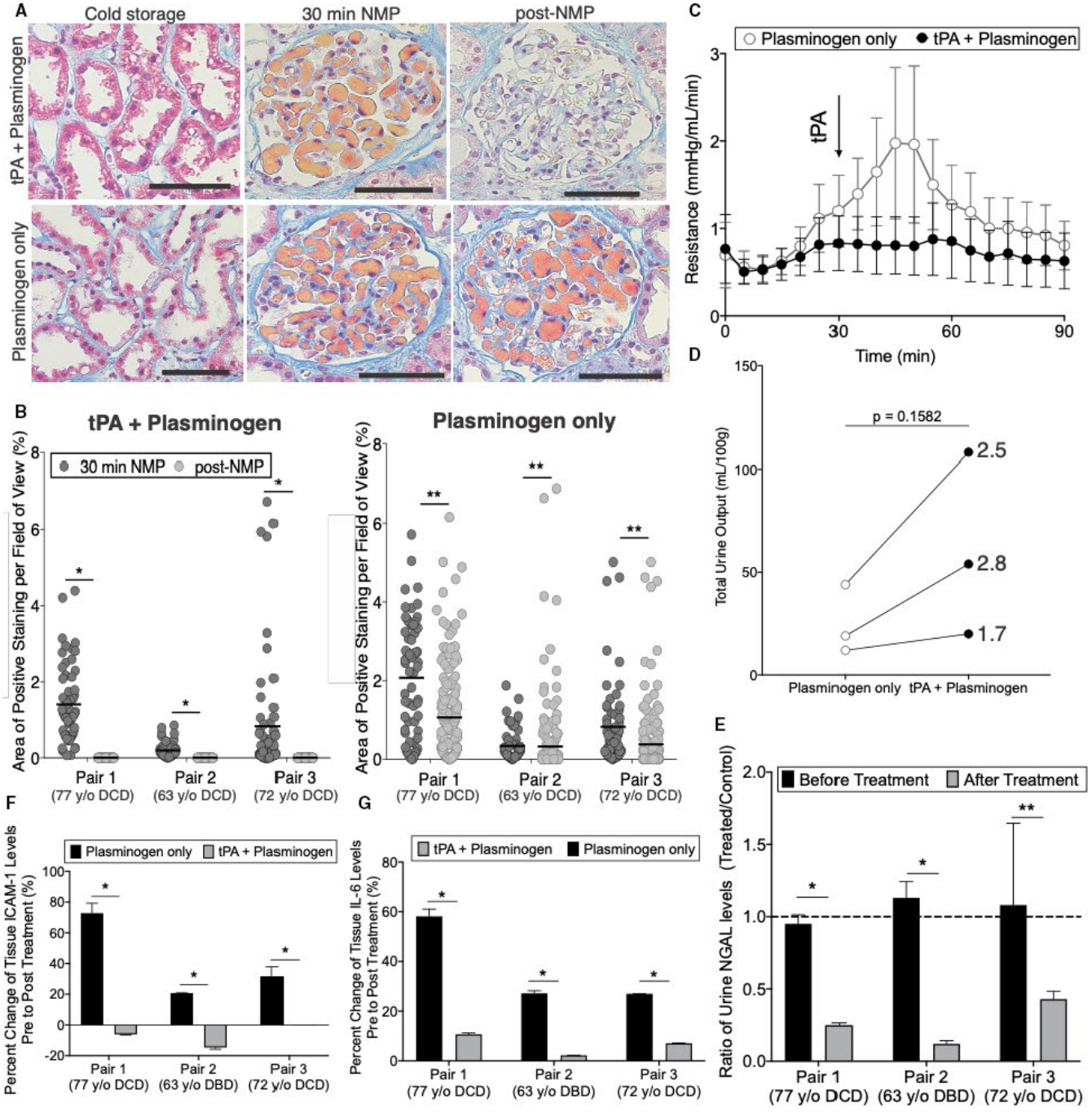


FIGURE 4 Paired donor organs suggest tissue plasminogen activator (tPA) + plasminogen treatment improves organ viability. A, Representative images and B, quantification of area of microvascular obstruction are shown for paired kidneys from the same donor treated with tPA + plasminogen or plasminogen only (*P < .0001, **P < .05; Mann-Whitney t test). Scale bars represent 100 µm. C, Resistance time traces as measured during normothermic machine perfusion (NMP) for plasminogen only vs tPA + plasminogen. Data points represent the mean and error bars signify standard error of the mean for each group of 3 kidneys. Arrow denotes point of tPA administration. D, Total urine output normalized to the mass of each kidney as measured after 90 min of NMP (*P = .1582; paired t test); lines connect paired organs from the same donor. E, Urine NGAL ratios of tPA + plasminogen relative to plasminogen only controls before and after treatment (*P < .00001, **P = .0188; multiple t tests). F, Soluble intercellular adhesion molecule 1 (ICAM-1; *P < .001; multiple t tests) and G, interleukin-6 (IL-6) levels as measured by ELISA on tissue lysates (*P < .00001; multiple t tests). Samples were processed in triplicate [Color figure can be viewed at wileyonlinelibrary.com]

In 2 older donors (Kidney 10 and 11 from the same 70 years old DBD; Kidney 12 from a 74-year-old DCD), we also observed an initial linear phase of fibrinogen increase within the first 24-30 hours. This was followed by a subsequent period of decay presumably because of cell death and subsequent enzymatic degradation (Figure 5B,C). The organs from the older donors had significantly faster rates of

16006143, 2021, 1, Downloaded from https://onlinelibrary.wiley.com/doi/10.1111/ajt.16148, Wiley Online Library on [25/10/2022]. See the Terms and Conditions (https://onlinelibrary.wiley.com/terms-and-conditions) on Wiley Online Library for rules of use; OA articles are governed by the applicable Creative Commons License

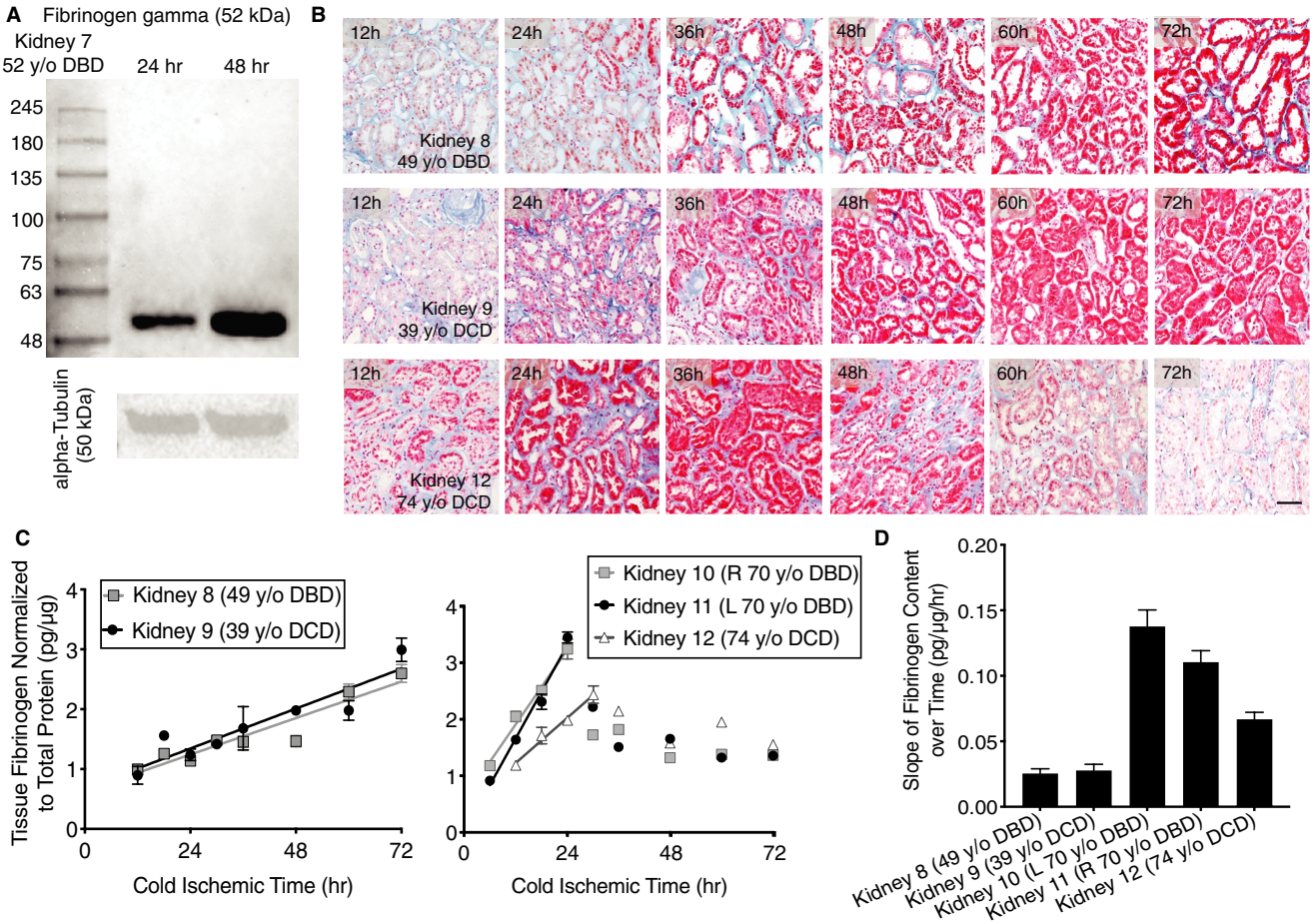


FIGURE 5 Tubular epithelia produce fibrinogen during cold storage at variable rates depending on the donor. A, Western blot depicting levels of fibrinogen gamma subunit and alpha-Tubulin loading controls from Kidney 7 at 24 and 48 h. B, Representative images of sections taken from repeat biopsy of a 49 y old donor after brain death (DBD), 39 y old donor after cardiac death (DCD), and 74 y old DCD kidneys over the course of 72 h. Martius scarlet blue (MSB) stain shows increasing fibrinogen accumulation in tubular epithelia during cold-storage (red). Scale bar represents 100 µm. C, Fibrinogen ELISAs performed on tissue lysates from repeat biopsies in 5 kidneys from 4 separate donors taken over the course of 72 h (left—younger donors; right—older donors). Lines represent a fit to the linear phase of fibrinogen production. D, Rate of fibrinogen production for each organ as derived from linear fits in (C). Error bars refer to standard deviation. All measurements were performed in technical triplicate [Color figure can be viewed at wileyonlinelibrary.com]

fibrinogen increase compared to the younger donors (Figure 5D). Within ~24-30 hours, the organs from older donors reached levels that took 72 hours to achieve in the organs from the younger donors.

3.6 | Lysing vascular obstructions improves specificity of vascular-targeted NPs

Based on our prior observations that microvascular obstructions impaired targeted NP delivery, we hypothesized that tPA + plasminogen treatment would enable more selective NP targeting.[13] To evaluate this, another series of 3 sequential pairs of nontransplanted donor organs were evaluated (Pair 4—77-year-old DBD; Pair 5—53-year-old DBD; and Pair 6—76-year-old DBD). Similar to the series described previously, the treated organs demonstrated improvements in stability of hemodynamics (Figure 6A), urine production (Figure 6B), and reduced NGAL as a marker of renal injury (Figure 6C).

In the absence of tPA + plasminogen treatment, there was no observed benefit of NP targeting when evaluated by 2-color quantitative microscopy as previously described.[13] The coadministered ICAM2-NPs (red) and Control-NPs (green) accumulated at identical levels presumably via a sieving mechanism at the site of vascular obstructions, as previously observed (Figure 6D,E).[13] However, in the paired kidney, the retention of the nontargeted Control-NP was significantly diminished in the absence of the microvascular obstructions. We observed ~3-fold enhanced retention of ICAM2-targeted NPs in the glomeruli ($P < .0001$) and ~20-fold benefit in the microvessels ($P < .0001$) (Figure 6E).

4 | DISCUSSION

The basic principles for successful preservation of organs for transplant were established during pioneering studies in the late

16006143, 2021, 1, Downloaded from https://onlinelibrary.wiley.com/doi/10.1111/ajt.16148, Wiley Online Library on [25/10/2022]. See the Terms and Conditions (https://onlinelibrary.wiley.com/terms-and-conditions) on Wiley Online Library for rules of use; OA articles are governed by the applicable Creative Commons License

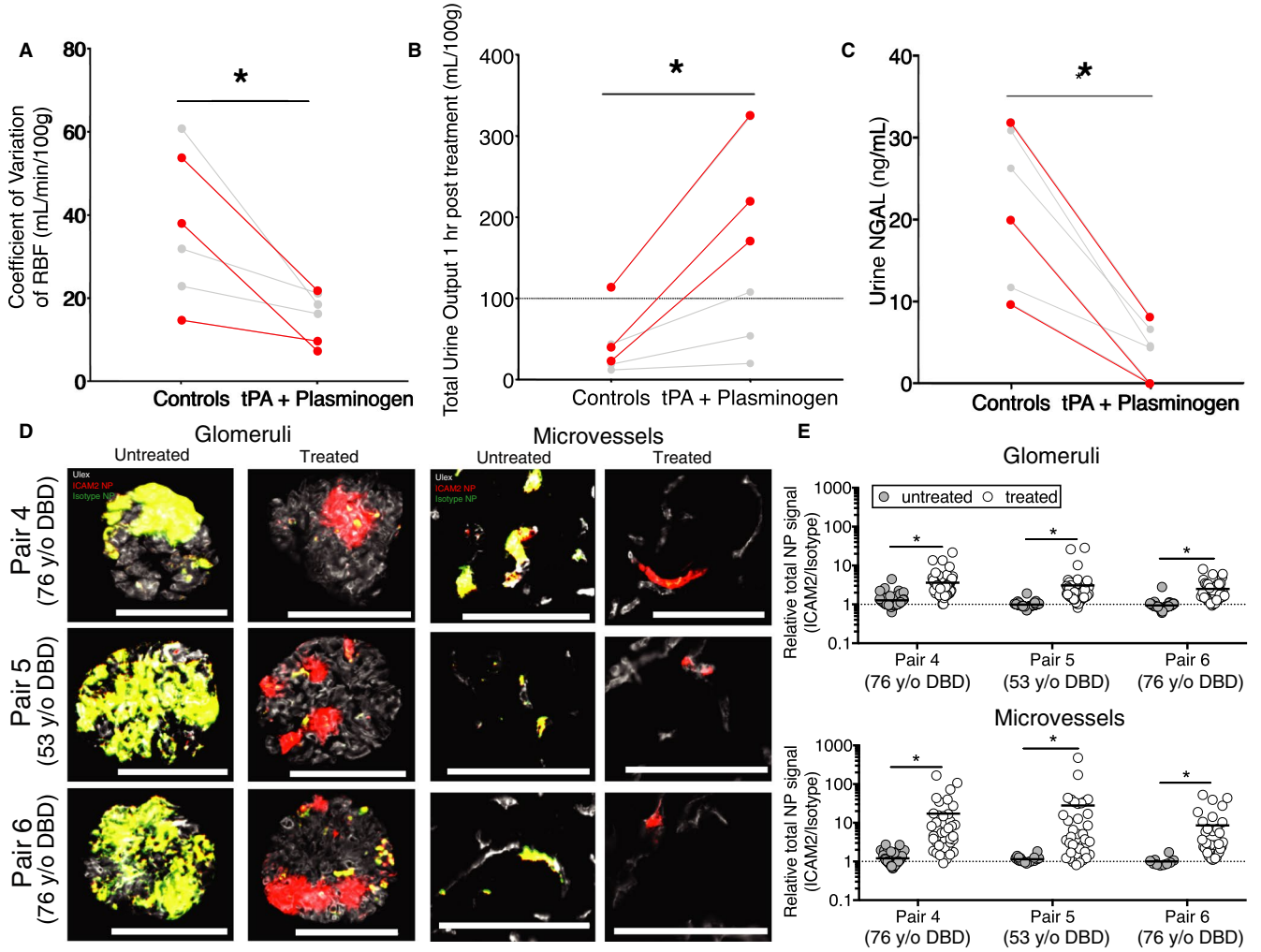


FIGURE 6 Lysing vascular obstructions improves specificity of vascular-targeted nanoparticles (NPs). A, Variation in renal blood flow (RBF) in tPA + plasminogen treated organs relative to paired controls as measured over the final 60 min of normothermic machine perfusion (NMP) (*P = .0126; paired t test). Each data point represents a single kidney and lines connect paired organs. Red data points and lines are from Pairs 4-6 that were stored for prolonged cold times of 30-36 h to build high fibrinogen levels. Gray data points and pairs refer to Pairs 1-3. B, Total urine production (*P = .0157; paired t test) and C, NGAL levels (*P = .0023; paired t test) over the final 60 min of NMP in treatment vs control groups. D, Representative images of glomeruli (left) and microvessels (right) from paired kidneys receiving either tissue plasminogen activator (tPA) + plasminogen treatment (treated) or NMP alone (untreated) prior to injection of combined intercellular adhesion molecule 2 (ICAM2)-NPs and Isotype-NPs labeled with 2 separate fluors (ICAM2-NPs, red; Isotype-NPs, green; NP-overlay, yellow; Ulex, white). E, Quantification of relative NP signal (ICAM2-NPs/Isotype-NPs) after 4 h of NP circulation. Each data point represents a separate image of either interstitial microvessels (top) or glomeruli (bottom); nonspecific (1:1) accumulation is represented by a dashed line (*P < .0001 Wilcoxon signed-rank test). Three separate sections were evaluated per kidney with 20 images per section collected for 60 images total per kidney. Scale bars represent 100 μm [Color figure can be viewed at wileyonlinelibrary.com]

1960s through late 1980s.[24-26] These efforts defined 5 key physiologic modes of failure that guided the design of preservation fluids to enable safe preservation of deceased-donor kidneys for ~24 hours.[24] However, these principles were established in an era with much less demand for organs and a generally healthier donor population. The poorer outcomes associated with more marginal donor organs prevalent today—even within the standard preservation cutoff times—suggests the possibility that there may be additional as yet unidentified modes of failure that need to be addressed to ensure these higher-risk organs can be safely preserved and transplanted.

Fortunately, our ability to perform preclinical research on the same nontransplanted organs that we aim to revitalize provides a unique opportunity to identify these additional failure modes. This discovery process is further aided by the capacity of NMP to simulate in vivo-like conditions in an isolated ex vivo setting. Here, NMP allowed us to identify that factors intrinsic to the kidney appear sufficient to elicit the observed microvascular obstructions. By eliminating the confounding source of hepatic fibrinogen, we were further able to identify the proximal tubular epithelium as the source of fibrin(ogen) contained within the observed microvascular obstructions.

16006143, 2021, 1, Downloaded from https://onlinelibrary.wiley.com/doi/10.1111/ajt.16148, Wiley Online Library on [25/10/2022]. See the Terms and Conditions (https://onlinelibrary.wiley.com/terms-and-conditions) on Wiley Online Library for rules of use; OA articles are governed by the applicable Creative Commons License

The low temperatures associated with cold storage (~4°C) are known to suppress cellular secretion. This sequestration appears to facilitate buildup of fibrinogen within the tubular epithelium that is then rapidly secreted into the urine and the microvasculature within 15 minutes upon restoration of normothermic temperatures. The mechanisms by which the fibrinogen enters the vasculature are unclear; however, there is evidence that proteins secreted into urine can be scavenged and translocated back into the microvasculature.[27-29] Regardless of the precise mechanism of transport, we posit that this rapid release of fibrinogen stores may contribute to the formation of RBC aggregates by creating high local concentrations of fibrinogen within the microenvironment of the peritubular capillaries. As there is continuous recirculation of blood in our closed-loop system, any RBC aggregates that do not immediately lodge in peritubular capillaries would continue to recirculate, which could account for the RBC obstructions detected in glomerular capillaries. Our observation that renal resistance levels typically begin to spike after ~15-30 minutes of NMP suggests that this is the critical window for lysis of these obstructions.

The fact that proximal tubular cells continue to produce fibrinogen under cold-storage conditions that significantly suppress metabolic activity suggests that fibrinogen likely plays an important role in the renal response to cold storage. Though fibrinogen synthesis is most commonly associated with the liver, extrahepatic production of fibrinogen has been previously observed, including in human kidneys.[30-33] These prior studies suggest that hypoxia can initiate extrahepatic fibrinogen production and that fibrinogen may have several additional functions outside of its known role in the clotting cascade.[34-36] Notably, multiple studies have demonstrated that a peptide fragment derived from the fibrinogen beta chain can actually be protective against renal ischemia reperfusion injury (IRI) in vivo.[34,37] However, knockout studies in mice suggest a complex role for fibrinogen in renal IRI with partial knockouts showing protective effects and full knockouts yielding exacerbated injury.[31,38]

A clear limitation of our current study is the fact that our data do not conclusively demonstrate that renal fibrinogen is sufficient to drive obstructions in the absence of other co-factors. Von Willebrand Factor, for example, has also been identified as a mediator of RBC-aggregation in the context of ischemia-reperfusion injury and is similarly sensitive to plasmin mediated degradation.[39,40] Thus, there is a clear need for a more detailed mechanistic investigation to complement the translational focus of this work. An additional limitation is the absence of posttransplant outcomes data to assess the clinical impact of the positive MSB stain observed in the patient samples in Figure 3. As this trial is still ongoing, we are currently unable to access these patients' records. However, this will be assessed at the conclusion of the trial anticipated in early 2021. We were also unable to assess any posttransplant benefits of our treatment regimen due to the use of nontransplanted human organs. This could be evaluated in a future preclinical study with a porcine model, presuming the same pathologic mechanism occurs in pigs. We also intend to perform a randomized control trial to directly assess clinical efficacy in human subjects.

Though there may well be alternatives to our combined tPA + plasminogen regimen, the utility of our approach lies in its capacity for immediate translation. tPA is a Food and Drug Administration (FDA)-approved therapeutic with a long history of clinical use in humans including in the setting of transplantation.[44,45] It should be noted that pretransplant treatment of kidneys with plasmin activating enzymes (eg, tPA and streptokinase) has previously been evaluated in both preclinical and clinical studies with mixed results.[41-43] However, these studies delivered these enzymes in the absence of the cofactor plasminogen, which our current study demonstrates is essential for complete fibrinolytic effect. Plasminogen is currently awaiting FDA approval as a replacement therapy for patients with plasminogen deficiency but has been shown in multiple clinical trials to also be safe for use in humans.[46-48] These prior clinical experiences should enable rapid translation of this approach for immediate improvement in utilization of marginal organs with longer cold-storage times. Furthermore, our results with nanoparticle delivery during NMP suggest that this approach could also represent an essential first step to enable subsequent use of the full toolkit of potential therapies for graft modification during NMP.

ACKNOWLEDGMENTS

The authors thank the donors and their families. Without their generous gifts, this study could not have been conducted. The authors also thank New England Donor Services for their assistance in providing organs for research. The authors thank Keziah Crick with the Cambridge Perfusion Team for her technical assistance in setting up the perfusions. The authors would also like to thank Ashley Priddey for his assistance with western blotting techniques and Dr Xinran Liu at the Center for Cellular and Molecular Imaging (CCMI), EM facility at Yale Medical School for their assistance with TEM imaging. The research was funded by the National Institute for Health Research Blood and Transplant Research Unit (NIHR BTRU) in Organ Donation and Transplantation at the University of Cambridge in collaboration with Newcastle University and in partnership with NHS Blood and Transplant (NHSBT). The views expressed are those of the authors and not necessarily those of the NHS, the NIHR, the Department of Health, or NHSBT. The research was also supported by the National Institutes of Health (Pober U01-AI32895; Tietjen R01-DK124420) and New England Donor Services (Haakinson and Tietjen).

DISCLOSURE

The authors of this manuscript have no conflicts of interest to disclose as described by the *American Journal of Transplantation*.

AUTHOR CONTRIBUTIONS

JD designed study, conducted perfusions, collected data, analyzed data, wrote paper; SA designed study, conducted perfusions, wrote paper. MR developed code to quantify microvascular obstructions, analyzed slides. C.A, L.B, formulated, conjugated nanoparticles CE assisted with perfusions AV collected data, JF BS MC analyzed data, wrote paper. DH, DM, WMS, JSP designed study, wrote paper. ST

16006143, 2021, 1, Downloaded from https://onlinelibrary.wiley.com/doi/10.1111/ajt.16148, Wiley Online Library on [25/10/2022]. See the Terms and Conditions (https://onlinelibrary.wiley.com/terms-and-conditions) on Wiley Online Library for rules of use; OA articles are governed by the applicable Creative Commons License

analyzed slides as a trained pathologist, MN, GT designed study, analyzed data, wrote paper.

DATA AVAILABILITY STATEMENT

Data available on request from the authors.

ORCID

Jenna R. DiRito https://orcid.org/0000-0002-8513-5937
Sarah A. Hosgood https://orcid.org/0000-0002-8039-143X
John R. Ferdinand https://orcid.org/0000-0003-0936-0128

REFERENCES

1. HHS. Organ Procurement and Transplantation Network. 2020. https://optn.transplant.hrsa.gov. Accessed May 11, 2020.
2. Bae S, Massie AB, Luo X, Anjum S, Desai NM, Segev DL. Changes in discard rate after the introduction of the kidney donor profile index (KDPI). *Am J Transplant*. 2016;16(7):2202-2207.
3. Cooper M, Formica R, Friedewald J, et al. Report of National Kidney Foundation Consensus Conference to decrease kidney discards. *Clin Transplant*. 2019;33(1):e13419.
4. Port FK, Merion RM, Roys EC, Wolfe RA. Trends in organ donation and transplantation in the United States, 1997–2006. *Am J Transplant*. 2008;8(4 Pt 2):911-921.
5. Hassanain M, Simoneau E, Doi SA, et al. Trends in brain-dead organ donor characteristics: a 13-year analysis. *Can J Surg*. 2016;59(3):154-160.
6. Le Dinh H, Monard J, Delbouille M-H, et al. A more than 20% increase in deceased-donor organ procurement and transplantation activity after the use of donation after circulatory death. *Transplant Proc*. 2014;46(1):9-13.
7. Stewart DE, Garcia VC, Rosendale JD, Klassen DK, Carrico BJ. Diagnosing the decades-long rise in the deceased donor kidney discard rate in the United States. *Transplantation*. 2017;101(3):575-587.
8. Hosgood SA, Saeb-Parsy K, Wilson C, Callaghan C, Collett D, Nicholson ML. Protocol of a randomised controlled, open-label trial of ex vivo normothermic perfusion versus static cold storage in donation after circulatory death renal transplantation. *BMJ Open*. 2017;7(1):e012237.
9. Nicholson ML, Hosgood SA. Renal transplantation after ex vivo normothermic perfusion: the first clinical study. *Am J Transplant*. 2013;13(5):1246-1252.
10. Hosgood SA, Nicholson ML. First in man renal transplantation after ex vivo normothermic perfusion. *Transplantation*. 2011;92(7):735-738.
11. DiRito JR, Hosgood SA, Tietjen GT, Nicholson ML. The future of marginal kidney repair in the context of normothermic machine perfusion. *Am J Transplant*. 2018;18(10):2400-2408.
12. Brasile L, Stubenitsky BM, Booster MH, Arenada D, Haisch C, Kootstra G. Transfection and transgene expression in a human kidney during ex vivo warm perfusion. *Transplant Proc*. 2002;34(7):2624.
13. Tietjen GT, Hosgood SA, DiRito J, et al. Nanoparticle targeting to the endothelium during normothermic machine perfusion of human kidneys. *Sci Transl Med*. 2017;9(418):eaam6764.
14. Brasile L, Henry N, Orlando G, Stubenitsky B. Potentiating renal regeneration using mesenchymal stem cells. *Transplantation*. 2019;103(2):307-313.
15. Hamilton PJ, Stalker AL, Douglas AS. Disseminated intravascular coagulation: a review. *J Clin Pathol*. 1978;31(7):609-619.
16. Lendrum AC, Fraser DS, Slidders W, Henderson R. Studies on the character and staining of fibrin. *J Clin Pathol*. 1962;15:401-413.
17. Merrill EW, Gilliland ER, Lee TS, Salzman EW. Blood rheology: effect of fibrinogen deduced by addition. *Circ Res*. 1966;18(4):437-446.
18. Wells RE Jr, Gawronski TH, Cox PJ, Perera RD. Influence of fibrinogen on flow properties of erythrocyte suspensions. *Am J Physiol*. 1964;207:1035-1040.
19. Maeda N, Seike M, Kume S, Takaku T, Shiga T. Fibrinogen-induced erythrocyte aggregation: erythrocyte-binding site in the fibrinogen molecule. *Biochim Biophys Acta*. 1987;904(1):81-91.
20. Roelofs J, Rouschop KMA, Teske GJD, et al. Endogenous tissue-type plasminogen activator is protective during ascending urinary tract infection. *Nephrol Dial Transplant*. 2009;24(3):801-808.
21. Tanaka T, Narazaki M, Kishimoto T. IL-6 in inflammation, immunity, and disease. *Cold Spring Harb Perspect Biol*. 2014;6(10):a016295.
22. Greenwald E, Yuki K. A translational consideration of intercellular adhesion molecule-1 biology in the perioperative setting. *Transl Perioper Pain Med*. 2016;1(2):17-23.
23. Shimizu Y, Minemura M, Tsukishiro T, et al. Serum concentration of intercellular adhesion molecule–1 in patients with hepatocellular carcinoma is a marker of the disease progression and prognosis. *Hepatology*. 1995;22(2):525-531.
24. Belzer FO, Southard JH. Principles of solid-organ preservation by cold storage. *Transplantation*. 1988;45(4):673-676.
25. Collins GM, Bravo-Shugarman M, Terasaki PI. Kidney preservation for transportation. *The Lancet*. 1969;294(7632):1219-1222.
26. Belzer FO, Ashby BS, Gulyassy PF, Powell M. Successful seventeen-hour preservation and transplantation of human-cadaver kidney. *N Engl J Med*. 1968;278(11):608-610.
27. Christensen EI, Birn H. Megalin and cubilin: multifunctional endocytic receptors. *Nat Rev Mol Cell Biol*. 2002;3(4):256-266.
28. Amsellem S, Gburek J, Hamard G, et al. Cubilin is essential for albumin reabsorption in the renal proximal tubule. *J Am Soc Nephrol*. 2010;21(11):1859-1867.
29. Baines RJ, Chana RS, Hall M, Febbraio M, Kennedy D, Brunskill NJ. CD36 mediates proximal tubular binding and uptake of albumin and is upregulated in proteinuric nephropathies. *Am J Physiol Renal Physiol*. 2012;303(7):F1006-F1014.
30. Hoffmann D, Bijol V, Krishnamoorthy A, et al. Fibrinogen excretion in the urine and immunoreactivity in the kidney serves as a translational biomarker for acute kidney injury. *Am J Pathol*. 2012;181(3):818-828.
31. Sörensen-Zender I, Rong S, Susnik N, et al. Role of fibrinogen in acute ischemic kidney injury. *Am J Physiol Renal Physiol*. 2013;305(5):F777-785.
32. Molmenti EP, Ziambaras T, Perlmutter DH. Evidence for an acute phase response in human intestinal epithelial cells. *J Biol Chem*. 1993;268(19):14116-14124.
33. Simpson-Haidaris PJ, Courtney MA, Wright TW, Goss R, Harmsen A, Gigliotti F. Induction of fibrinogen expression in the lung epithelium during Pneumocystis carinii pneumonia. *Infect Immun*. 1998;66(9):4431-4439.
34. Krishnamoorthy A, Ajay AK, Hoffmann D, et al. Fibrinogen beta-derived Bbeta(15–42) peptide protects against kidney ischemia/reperfusion injury. *Blood*. 2011;118(7):1934-1942.
35. Palumbo JS, Degen JL. Hemostatic factors in tumor biology. *J Pediatr Hematol Oncol*. 2000;22(3):281-287.
36. Adams RA, Schachtrup C, Davalos D, Tsigelny I, Akassoglou K. Fibrinogen signal transduction as a mediator and therapeutic target in inflammation: lessons from multiple sclerosis. *Curr Med Chem*. 2007;14(27):2925-2936.
37. Sorensen I, Rong S, Susnik N, et al. Bbeta(15–42) attenuates the effect of ischemia-reperfusion injury in renal transplantation. *J Am Soc Nephrol*. 2011;22(10):1887-1896.
38. Ajay AK, Saikumar J, Bijol V, Vaidya VS. Heterozygosity for fibrinogen results in efficient resolution of kidney ischemia reperfusion injury. *PLoS One*. 2012;7(9):e45628.

16006143, 2021, 1, Downloaded from https://onlinelibrary.wiley.com/doi/10.1111/ajt.16148, Wiley Online Library on [25/10/2022]. See the Terms and Conditions (https://onlinelibrary.wiley.com/terms-and-conditions) on Wiley Online Library for rules of use; OA articles are governed by the applicable Creative Commons License

39. Nicolay JP, Thorn V, Daniel C, et al. Cellular stress induces erythrocyte assembly on intravascular von Willebrand factor strings and promotes microangiopathy. *Sci Rep*. 2018;8(1):10945.
40. Smeets MWJ, Mourik MJ, Niessen HWM, Hordijk PL. Stasis promotes erythrocyte adhesion to von Willebrand factor. *Arterioscler Thromb Vasc Biol*. 2017;37(9):1618-1627.
41. Gok MA, Shenton BK, Peaston R, et al. Improving the quality of kidneys from non-heart-beating donors, using streptokinase: an animal model. *Transplantation*. 2002;73(12):1869-1874.
42. Woodside KJ, Goldfarb DA, Rabets JC, et al. Enhancing kidney function with thrombolytic therapy following donation after cardiac death: a multicenter quasi-blinded prospective randomized trial. *Clin Transplant*. 2015;29(12):1173-1180.
43. A Gok M, Shenton BK, Buckley PE, et al. How to improve the quality of kidneys from non-heart-beating donors: a randomised controlled trial of thrombolysis in non-heart-beating donors. *Transplantation*. 2003;76(12):1714-1719.
44. Seal JB, Bohorquez H, Reichman T, et al. Thrombolytic protocol minimizes ischemic-type biliary complications in liver transplantation from donation after circulatory death donors. *Liver Transpl*. 2015;21(3):321-328.
45. Hashimoto K, Eghtesad B, Gunasekaran G, et al. Use of tissue plasminogen activator in liver transplantation from donation after cardiac death donors. *Am J Transplant*. 2010;10(12):2665-2672.
46. Shapiro AD, Nakar C, Parker JM, et al. Plasminogen replacement therapy for the treatment of children and adults with congenital plasminogen deficiency. *Blood*. 2018;131(12):1301-1310.
47. Tefs K, Gueorguieva M, Klammt J, et al. Molecular and clinical spectrum of type I plasminogen deficiency: a series of 50 patients. *Blood*. 2006;108(9):3021-3026.
48. Plasminogen Deficiency. https://liminalbiosciences.com/pipeline/plasminogen/plasminogen-deficiency-clinical-trials/. Accessed March 20, 2020.

SUPPORTING INFORMATION

Additional supporting information may be found online in the Supporting Information section.

How to cite this article: DiRito JR, Hosgood SA, Reschke M, et al. Lysis of cold-storage-induced microvascular obstructions for ex vivo revitalization of marginal human kidneys. *Am J Transplant*. 2021;21:161–173. https://doi.org/10.1111/ajt.16148

16006143, 2021, 1, Downloaded from https://onlinelibrary.wiley.com/doi/10.1111/ajt.16148, Wiley Online Library on [25/10/2022]. See the Terms and Conditions (https://onlinelibrary.wiley.com/terms-and-conditions) on Wiley Online Library for rules of use; OA articles are governed by the applicable Creative Commons License